Original Research Article

Comparative Corrosion Inhibition Ability of Triphenylphosphine and Its Derivatives on Aluminum Surfaces Using Computational Approach

Fater Iorhuna[1], *, Abdullahi Muhammad Ayuba[1], Thomas Aondofa Nyijime[2]

[1]*Department of Pure and Industrial Chemistry, Faculty of Physical Sciences, Bayero University, Kano, Nigeria*
[2]*Department of Chemistry, Joseph Sawuan Tarka University, Makurdi, Benue, Nigeria*

Use yor device to scan and read the article online

Citation F. Iorhuna, A.M. Ayuba, T.A. Nyijime Comparative Corrosion Inhibition Ability of Triphenylphosphine and Its Derivatives on Aluminum Surfaces Using Computational Approach. *J. Eng. Ind. Res.* **2025**, 6 (1):33-52.

https://doi.org/10.48309/jeires.2025.500901.1154

Article info:
Submitted: 2025-01-19
Revised: 2025-02-18
Accepted: 2025-03-04
ID: JEIRES-2501-1154

Keywords:
PDP; Simulation; Aluminum; Triphenylphosphine; Corrosion; Mechanism

ABSTRACT

This study evaluates the corrosion inhibition potential of three molecules—TPP, TBP, and TFP—by analyzing their electronic properties and interaction energies with aluminum surfaces (Al (111), Al (110), and Al (100)). Key electronic parameters such as the Energy of Highest Occupied Molecular Orbital (E-HOMO), Energy of Lowest Unoccupied Molecular Orbital (E-LUMO), Ionization Energy (IE), Electron Affinity (AE), and Energy Gap (ΔEg) reveal that TPP is the most effective electron donor, followed by TFP and TBP, which is a stronger electron acceptor. Kinetic and potential energy simulations indicate that TBP exhibits the most negative potential energy values, particularly on Al (100), suggesting the strongest interaction with the aluminum surfaces and superior inhibition performance. In contrast, TFP shows stronger interaction with Al (100) but weaker binding on Al (110) and Al (111), while TPP displays the weakest interaction overall. Kinetic energy results indicate that TBP induces the highest molecular movement on Al (100), reflecting more dynamic interactions, whereas TFP induces moderate energy levels with less variation across surfaces. The potential energy values, all negative, suggest attractive interactions between the inhibitors and the aluminum surfaces. TBP exhibits the most negative values, followed by TFP and TPP, indicating that TBP likely forms the strongest bonds with aluminum. These findings suggest that TBP is the most effective corrosion inhibitor, especially for Al (100), while TFP and TPP show varying levels of effectiveness based on their interactions with the different aluminum surfaces. Simulations were conducted using force field dynamic energies, offering insights into the molecular behaviors and their potential for corrosion inhibition.

***Corresponding Author: Fater Iorhuna** (uyerfater22@gmail.com)*

Introduction

Aluminum, a widely used lightweight metal, plays a crucial role in various industries, including aerospace, automotive, construction, and electronics [1-4]. Despite its inherent resistance to corrosion, aluminum is still susceptible to corrosion under certain conditions, such as exposure to chloride ions, acidic environments, and high humidity [5]. Metals of the group, including aluminum, gallium, indium, and thallium, exhibit varying behaviors towards corrosion in acidic environments [6]. Aluminum is highly reactive but forms a protective oxide layer (Al_2O_3) that shields it from further corrosion in mild acidic conditions. However, in stronger acids, the oxide layer can be dissolved, leading to increased corrosion. This vulnerability poses significant challenges in maintaining the metal's physical properties and extends its life-span [7]. As a result, the development of effective corrosion inhibitors has become an essential area of research on the aluminum and other metals of importance. The phosphorus atom in triphenylphosphine (TPP) has a lone pair of electrons, which could coordinate with metal ions on the surface of aluminum. This could, in theory, form a protective barrier on the metal surface, preventing further corrosion by blocking the interaction between the metal and corrosive agents (e.g., oxygen, water, and acidic species). Phosphine compounds are sometimes known to form thin phosphide layers on metal surfaces, which could help passivate the surface [8]. Triphenylphosphine (TPP) and its derivatives are organophosphines a versatile organic phosphorus compound with a wide range of applications, especially in organic synthesis and as a ligand in coordination chemistry [9,10]. Triphenylphosphine's function as an inhibitor is primarily due to its ability to interact with other molecules via its phosphorus atom. The phosphorus center can act as a nucleophile, donating its lone pair of electrons to electrophilic species, such as metal ions, transition states, or other reactive centers in biological or chemical systems [11,12]. The relationship between Triphenylphosphine (TPP), Tris-(4-bromo-phenyl)-phosphine (TBP), and Tris-(4-fluorophenyl)-phosphine (TFP) lies in how the electron-withdrawing substituents (bromine and fluorine) affect the electron density on the phosphorus atom, enhancing its ability to interact with and adsorb onto metal surfaces. The more electrophilic phosphorus becomes, the stronger its bond with the metal, improving the corrosion inhibition efficiency. Of these compounds, Tris-(4-fluorophenyl)-phosphine (TFP) is expected to exhibit the highest corrosion resistance due to the combined effects of strong electron-withdrawing fluorine atoms and the enhanced ability to form a durable and stable protective layer on the metal surface. These molecules possess unique electronic properties, making it attractive molecules for corrosion inhibition. Previous studies on the corrosion inhibition of aluminum have not focused on comparing the studied molecules on the surface of aluminum metal. The effectiveness of these inhibitors is often evaluated by their ability to reduce corrosion rates in aggressive environments, especially in the presence of chloride ions. However, the comparison of TPP, TBP, and TFP on the surface of aluminum metal has not been explored using computational methods such as DFT and molecular dynamics simulations. In case of Triphenylphosphine, previous experimental studies have demonstrated its potential as a corrosion inhibitor for various metals, including mild steel, copper, and aluminum. These studies generally observe that TPP may act by adsorbing onto the metal surface through both electrostatic and chemical interactions, possibly by forming complexes with metal cations or creating a physical barrier to corrosive species. These existing studies are largely experimental, relying on electrochemical techniques such as potentiodynamic polarization, weight loss measurements, and surface characterization methods like scanning electron microscopy (SEM) and X-ray photoelectron spectroscopy (XPS). While these techniques provide valuable insights into the macroscopic effects of the inhibitor, they fall short of explaining the microscopic and atomic-level interactions that underpin the corrosion inhibition process. Furthermore, these experimental methods are often time-consuming and may require

sophisticated equipment's that are not readily available in all laboratories. Moreover, experimental studies often face challenges in controlling environmental variables such as temperature, humidity, and electrolyte concentration, which can introduce inconsistencies in the results. The interpretation of these results is further complicated by the difficulty in directly observing the adsorption process and the formation of protective films. In addition, the influence of the chemical structure of the relationship between Triphenylphosphine (TPP), Tris-(4-bromo-phenyl)-phosphine (TBP), and Tris-(4-fluorophenyl)-phosphine (TFP) on inhibition efficiency are not fully explored, or compare on the aluminum metal. To overcome these limitations, computational methods, such as Density Functional Theory (DFT) and molecular dynamics simulations, offer a promising alternative. These techniques can provide a more detailed understanding of the molecular interactions between TPP and its derivatives and the aluminum surface, allowing researchers to explore a wide range of conditions *in silico* before conducting expensive and time-consuming experiments. The aim of this study is to examine the molecular interactions and adsorption mechanisms, focusing on the adsorption process of TPP, TBP, and TFP molecules on aluminum surfaces. It aims to determine whether physisorption or chemisorption occurs. The study calculated the energy profile of the adsorption process, including adsorption energy (ΔE) and the interaction energy between TPP, TBP, TFP, and aluminum atoms. Using DFT (Density Functional Theory) or molecular simulations, the most stable configurations of TPP on the aluminum surface will be predicted. Furthermore, the TPP effect on the electrochemical potential of the aluminum surface will be analyzed, exploring how it may reduce the surface's susceptibility to corrosion. Molecular dynamics simulations will be employed to predict TPP's behavior at the atomic level, focusing on its interaction with the aluminum surface and the surrounding environment over time. Moreover, this study aims to compare the efficacy of triphenylphosphine with other known corrosion inhibitors, and it also tries to compare the binding energies and extent of inhibition of TPP with those of other inhibitors to identify whether TPP outperforms others in terms of corrosion prevention efficiency. The structure in Scheme 1 present the molecules studied in this study.

Methods

Density functional theory

The method use in this study is similar to the methods used by [13,14] in line with the extended Koopman's theorem, which help to elucidate the initial electron distribution and local reactivity, particularly the Fukui function f(r), via ab-initio quantum chemistry methods [15-17]. Prior to calculate the stable geometries, the molecules were designed using ChemDraw Ultra 7.0.3 by Cambridge Software [18]. The result obtained was subjected to Equations (1-14) to obtain the local and global parameters of the molecules.

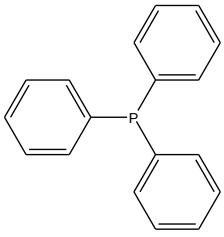

Triphenyl-phosphane

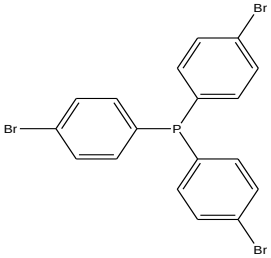

Tris-(4-Fluorophenyl)phosphine

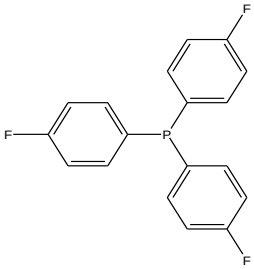

Tris-(4-Fluorophenyl)phosphine

Scheme 1: Structure of the molecules and its derivatives.

IE: Ionization energy (eV) $IE = -E_{HOMO}$ (1)

AE: Electron affinity (eV) $AE = -E_{LUMO}$ (2)

ΔE_g: Energy gap (eV) $\Delta E_g = E_{LUMO} - E_{HOMO}$ (3)

χ: absolute electronegativity (eV) $\chi = \frac{IE+AE}{2} = -\frac{(E_{HOMO}+E_{LUMO})}{2}$ (4)

η: global hardness (eV) $\eta = \frac{IE-AE}{2} = \frac{(E_{LUMO}-E_{HOMO})}{2}$ (5)

σ: global softness $(eV)^{-1}$ $\sigma = \frac{1}{\eta} = -\frac{2}{E_{HOMO}-E_{LUMO}}$ (6)

ω: global electrophilicity index (eV) $\omega = \frac{\mu^2}{2\eta} = \frac{\chi^2}{2\eta}$ (7)

μ: chemical potential (Debye) $\mu \approx -\frac{1}{2}(IE + AE) = \frac{1}{2}(E_{LUMO}+E_{HOMO})$ (8)

□: nucleophilicity $(eV)^{-1}$ $\varepsilon = \frac{1}{\omega}$ (8)

ΔE_{b-d}: Energy of back donation $\Delta E_{b-d} = -\frac{\eta}{4} = \frac{1}{8}(E_{HOMO} - E_{LUMO})$ (9)

ΔN: Fraction of electron(s) transfer $\Delta N = \frac{\chi Me - \chi Inh.}{2(\square Me + \square Inh)}$ (10)

$f(k)^+ = qk(N+1) - qk(N)$ (for nucleophilic attack) (11)

$f(k)^- = qk(N) - qk(N-1)$ (for electrophilic attack) (12)

$f(k)^0 = \frac{qk(N+1)-qk(N-1)}{2}$ (for radical attack) (13)

$\Delta f(k) = f^+ - f^- = f^2$ (Fukui function) (14)

Where, the absolute hardness (ηinh) and absolute electronegativity (χinh) of the inhibitor molecule are similar to those of aluminum. Theoretically, the global hardness of aluminum surfaces is 0 eV, and the electronegativity of aluminum is χAl = 5.6 eV, assuming that metallic bulk has a higher density compared to neutral metallic atoms [19-23]. The difference between nucleophilic and electrophilic local Fukui functions is defined by the Fukui second function (f2), also known as the dual descriptor Δf(k). These functions, which are derived from the Fukui behavior of atoms, indicate whether a molecule is more likely to undergo electrophilic or nucleophilic attacks [24,25]. Specifically, if f2(r) > 0, the site k is more likely to be attacked nucleophile, while if f2(r) < 0, it is more prone to electrophilic attack. Thus, f2(r) acts as a selectivity index for identifying the nature of the attacks. In this context, N represents the total number of electrons in the molecule, while N+1 denotes an anion formed by adding an electron to the Lowest Unoccupied Molecular Orbital (LUMO) of the neutral molecule, and N-1 signifies a cation formed by removing an electron from the Highest Occupied Molecular Orbital (HOMO) of the neutral molecule. The variable qk represents the net charge of atom k within the molecule, reflecting the electron density at a specific point r in space surrounding the molecule. The initial ground state geometry was utilized as the reference point for all subsequent calculations. Employing an atomic charge partitioning method, such as Mulliken population analysis outlined in Equations, these functions were concentrated on the nuclei of the atoms [26,27].

Molecular dynamic simulations

To replicate the behaviour of the TPP and its derivatives molecule on Al (110) surfaces, a quench adsorption method with high stability was used. This simulation was carried out using the FORCITE tool package within BIOVIA Materials Studio 8.0 (Accelrys, Inc.), utilizing the COMPASS force field and the Smart algorithm approach in a simulation box of 17Å x 12Å x 28Å to represent a typical surface area [28]. The Al crystals were modelled with (110) planes at a fractional depth of 3.0 Å, with the bottom layers fixed to reduce edge effects from molecular sizes before surface optimization. A 3x3 super-cell was created by extending the

surfaces. To balance the kinetic energy, a temperature of 350 K was maintained, preventing excessive desorption or hindered molecular movement across the surface [11,19,29]. The simulation was run for 5 ps with a time step of 1 fs, using the NVT (micro-canonical) ensemble to regulate temperature. Quenching was performed every 250 steps over 5000 cycles to ensure the statistical accuracy of the energy values on the aluminium crystal surfaces. The FORCITE tool was used to determine the lowest energy interactions between the molecules and Al (110) surfaces through geometry optimization [30-35]. Equations (15-16) were utilized to calculate the adsorption and binding energies of the Acridine, and its derivative-aluminium surface.

$$E_A = E_T - (E_I + E_S) \quad (15)$$

$$E_B = - E_A \quad (16)$$

Where, E_A is the adsorption energy, E_T is the combined energy of the molecule and the iron surface, E_S is the energy of the iron surface, E_I is the energy of the inhibitor molecule without the iron surface and E_B is the binding energy [36].

Results

Density functional theory

Table 1 provides important electronic properties related to the corrosion inhibition strength of the three molecules: TPP, TBP, and TFP. These properties offer significant insights into their potential interactions with the metal surface, especially in terms of electron transfer and adsorption, which provide inhibition efficiency on the surfaces.

Energy of Highest Occupied Molecular Orbital (E-HOMO) and Energy of Lowest Unoccupied Molecular Orbital (E-LUMO)

The molecule's capacity to give or receive electrons can be inferred from its HOMO and LUMO energies. According to Boulhaoua *et al.* [5], TPP has the greatest HOMO energy (-5.75 eV) of the three molecules generated from TPP, indicating that it is the most probable molecule to transfer electrons to the metal surface, hence preventing corrosion on the surfaces. TPP may take electrons from the metal surface during the inhibition process since it has the greatest LUMO energy (-0.51 eV). On the other hand, TBP appears to be less successful in electron donation and may not interact more efficiently on the metal surface than TPP or TFP, as evidenced by its lowest HOMO energy (-6.19 eV) and LUMO energy (-1.13 eV).

Ionization energy (I) and electron affinity (A)

A compound's oxidation and reduction potential can be used to show its anticorrosion ability. This is predicated on the compound's electron affinity (A) and ionization potential (I). Because it is quickly oxidized, a molecule with a low I value serves as an excellent electron donor [23]. TPP is simpler to ionize than TBP (6.19 eV), which has a higher ionization energy value, since it has a lower ionization energy (5.75 eV). TPP's electron affinity is the lowest at 0.51 eV, meaning it is less likely to receive electrons than TBP (1.13 eV). This might indicate that TPP functions largely as a donor, whereas TBP may be more of an acceptor of electrons [25,26].

Energy Gap (ΔEg)

A molecule's stability can be inferred from the energy difference between its HOMO and LUMO. A molecule that has a greater energy gap is more stable and has a lower potential to interact with the metal surface [1-3,27]. TFP is projected to be the least reactive due to its largest energy gap (5.28 eV) [10]. Because they can more easily engage in electron donation or back donation, TPP and TBP appear to be more reactive and effective at inhibiting corrosion, as evidenced by their slightly smaller energy gaps (5.24 eV and 5.06 eV, respectively) [23].

Electronegativity (χ)

TBP has the highest electronegativity (3.66 eV) of the three molecules, indicating that it has a stronger tendency to accept electrons from the metal surface. This ability boosts the molecule's capacity to form stable bonds with

the metal, preventing the metal from undergoing further oxidation or corrosion. This ability to accept electrons from the metal surface is especially important in the context of corrosion inhibition. A greater electronegativity denotes a stronger electron-accepting capacity, which is essential for corrosion inhibition, according to John et al. and Al-Joborry *et al.* [35,36]. By removing electrons from the metal surface in this situation, TBP may create a strong bond and lessen the metal's susceptibility to corrosive substances. Because it stabilizes the metal surface by decreasing its reactivity, its electron-accepting properties may improve its capacity to prevent corrosion. Compared to TBP, TPP and TFP are less able to receive electrons due to their lower electronegativity values (2.62 eV for TPP and 2.53 eV for TBP). Accordingly, the metal surface is less likely to be stabilized by TPP and TFP's contact through electron acceptance, even if they may still interact with the metal. They therefore play a more dependent role in inhibiting corrosion through different processes, such as electron donation (for TPP) as opposed to electron uptake (for TBP).

Hardness (η)

A higher hardness indicates that the molecule is less likely to give or take electrons readily, indicating that it is more stable and less susceptible to reactive interactions. The molecule's capacity to interact with the metal surface may be impacted by its stability when it comes to corrosion inhibition. Of the three compounds, TFP is the most stable and has the highest global hardness (2.64 eV). Higher hardness compounds are often less reactive, which means they are less likely to donate or receive electrons, as suggested in [32-35]. Because of its decreased reactivity, TFP may be less effective in inhibiting corrosion because it is less able to establish robust contacts with the metal surface. TFP is stable, however its capacity to block may be limited by its lack of reactivity with the metal surface. In this instance, the higher reactivity of TPP and TBP indicates that these molecules are better able to form bonds with the metal surface, improving their ability to inhibit corrosion. Softer molecules are more likely to interact with metal surfaces because they are more likely to either donate or accept electrons, depending on the needs of the surface.

Softness (σ) and Electrophilicity Index (ω)

The softness (σ) indicates how easily a molecule can accept electrons, and the electrophilicity index (ω) reflects the molecule's ability to accept electrons [37]. TBP has the highest softness (0.3953 eV-1), suggesting that it is more reactive and can more easily interact with the metal surface [1-5,37-40]. Its higher electrophilicity index (2.6473 eV) further supports electrophilicty result indicating that it is a strong electron acceptor. TPP (0.3816 eV^{-1} and 1.8696 eV) and TFP (0.3788 eV^{-1} and 2.0876 eV) are less electrophilic, suggesting less reactivity in accepting electrons according to Madkour and Elshamy and Ayuba *et al.* [41,42].

Nucleophilicity (ε)

Nucleophilicity measures the tendency of a molecule to donate electrons to an electrophile [17,37]. TPP has the highest nucleophilicity (0.5349), suggesting that, it will be the most effective in donating electrons to the metal surface, supporting its role as an anodic inhibitor [43,44]. TFP (0.4790) and TBP (0.3777) have lower nucleophilicity, with TBP being the least effective in this regard [30,45].

Energy of back donation (ΔEb-d)

Back Donation Energy (ΔEb-d) is the energy released when a metal center, usually a transition metal, donates electrons from its filled d-orbitals into the empty π* (anti-bonding) orbitals of a ligand. This process is commonly called the back-donation process and is crucial for stabilizing the metal-ligand complex. ΔEb-d is a key component of metal-ligand interactions, and the stability of the metal-ligand complex can be impacted by an inhibitor that interacts with the metal center in a way that either enhances or interferes with the back donation of electrons. In contrast, a lower ΔEb-d would indicate weaker back

donation, destabilizing the metal-ligand interaction and possibly making the complex more susceptible to inhibition. TFP has the most negative ΔEb-d (-0.6600), suggesting a stronger back donation, according to Belghiti *et al.* and Nyijime *et al.* [37,47]. A higher ΔEb-d indicates a more stable metal-ligand interaction because the metal center can donate more electron density into the ligand, which could improve catalysis or the complex's effectiveness.

Fraction of electron transfer (ΔNFe)

The proportion of electron transfer that takes place in a coordination complex between the metal center and the ligand or substrate is denoted as ΔNFe (proportion of Electron Transfer). It measures the amount of electron density that is moved from the metal center to the ligand when the complex is formed or activated. Following TPP (-0.6550) and TBP (-0.6325), this percentage can be affected by the ligand, metal, and environmental factors [17]. The amount of electron transfer from the inhibitor to the metal is shown by the percentage of electron transfer (ΔNAl) [44-50]. TPP has the greatest electron transfer percentage (0.4713), indicating the most efficient contact with the metal surface.

Figure 1 displays the LUMO Map which indicates the regions of a molecule most likely to accept electrons from the metal surface, these highlight the molecules potential as an electron acceptor. Electron density distribution reveals how electrons are spatially distributed across the molecule, influencing its reactivity and interaction with the metal. Likewise, the optimized geometry of the molecule in this figure provides the most stable molecular arrangement, crucial for understanding how the inhibitor interacts with the metal surface during corrosion inhibition. The local ionization potential which represents the molecule's ability to lose electrons locally and aids in identifying the sites most likely to donate electrons during the corrosion process is presented in the figure.

Table 1: Global energies of the inhibitor molecules

Energy	TPP	TBP	TFP
E-HOMO	-5.75	-6.19	-5.96
E-LUMO	-0.51	-1.13	-0.68
IE: Ionization energy (eV) IE	5.75	6.19	5.96
AE: Electron affinity (eV)	0.51	1.13	0.68
ΔEg: Energy gap (eV) ΔEg	5.24	5.06	5.28
χ: absolute electronegativity (eV)	3.13	3.66	3.32
η : global hardness (eV)	2.62	2.53	2.64
σ: global softness (eV)-1	0.3816	0.3953	0.3788
ω: global electrophilicity index (eV	1.8696	2.6473	2.0876
ε:nucleophilicity	0.5349	0.3777	0.4790
ΔEb-d: Energy of back donation	-0.6550	-0.6325	-0.6600
Dipole	1.42	0.69	0.07
ΔNFe: Fraction of electron(s) transfer	0.4713	0.3834	0.4318

Table 2: Forcite dynamic energy of the molecule after simulation

TPP		Al(111)	Al(110	Al(100)
Total Kinetic Energy		21.057±0.01	20.741±0.02	22.836±0.4
Total Potential Energy		-27.439±0.01	-20.479±0.02	-22.261±0.4
TBP				
Total Kinetic Energy		23.472±0.0	20.503±0.5	31.879±0.1
Total Potential Energy		-50.995±0.0	-41.843±0.5	-42.330±0.1
TFP				
Total Kinetic Energy		26.233±0.0	24.214±0.5	27.232±1.1
Total Potential Energy		-35.2225±0.0	-30.222±0.5	-45.225±1.1

TPP TBP TFP

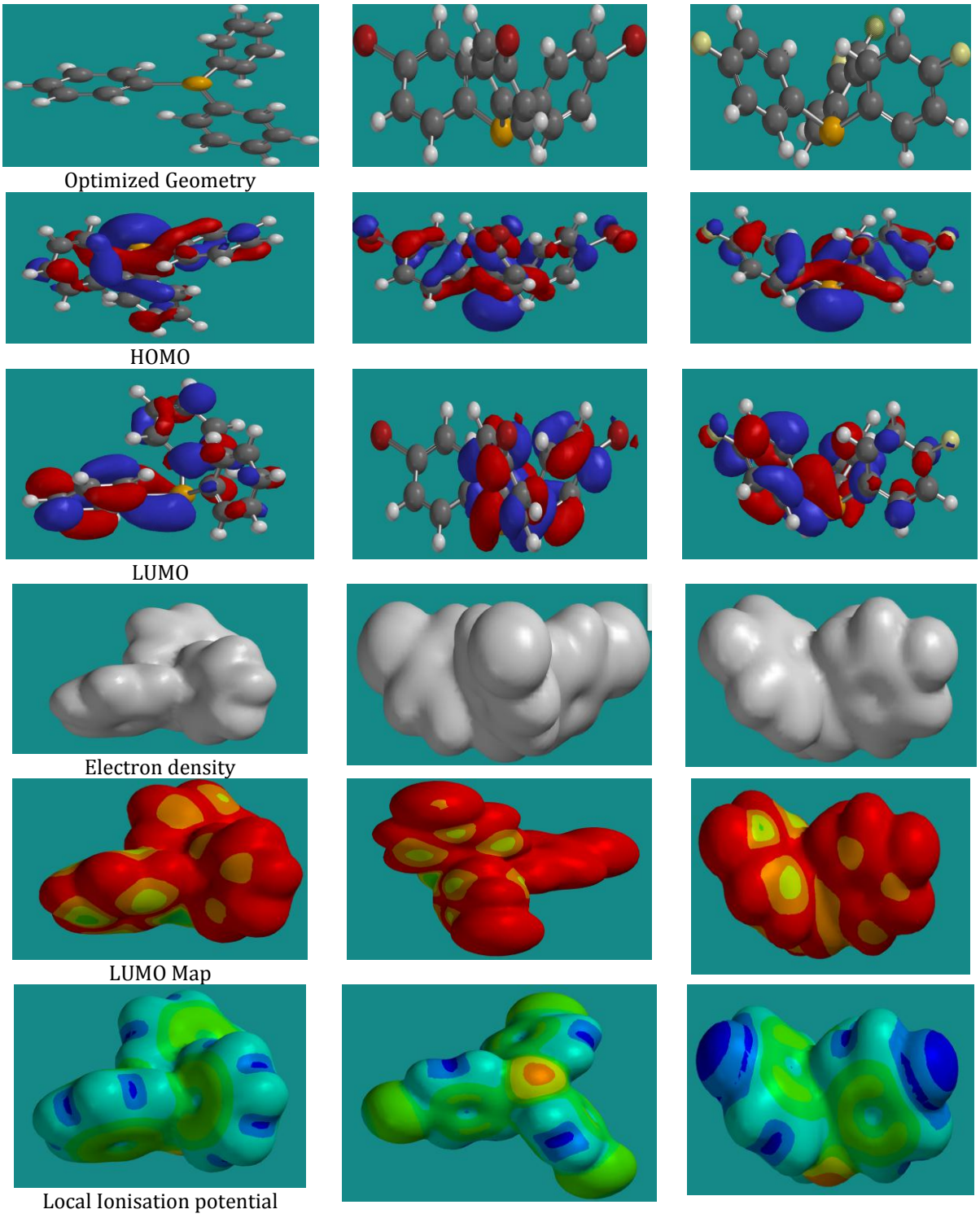

Figure 1: The short form of the molecules presenting LUMO Map, electron density, and local ionization potential.

Dynamic simulation

Forcite is a molecular simulation tool that calculates molecular properties using force-field methods. A force field is a set of equations and parameters that describe the potential energy of a system based on the positions of atoms. In dynamic simulations, the movement of atoms over time is tracked, and their interactions are evaluated [51]. The term "dynamic energy" encompasses several energy contributions within a molecular system such as Kinetic Energy: which is associated with the motion of atoms or molecules (for example, in the context of corrosion inhibition on metal surfaces). Potential energy includes energy from interactions between atoms (such as bonds, angles, and dihedrals), non-bonded interactions (like van der Waals forces and electrostatics), and other contributions like solvation energy [17,47,52-54]. Dynamic energy simulations can track how energy changes as reactants convert to products. This helps identify activation energies and assess the feasibility of a reaction at a given temperature. For larger molecules, tracking dynamic energy can reveal how energy is distributed during conformational changes (such as folding/unfolding or ligand binding). The energy fluctuations during these processes provide information about the stability or instability of various conformations [55]. The result of the potential and kinetic energy of the molecules TPP, TBP, and TFP are presented in Figures 2 and 3.

Figures 2 and 3 depict the potential energy and kinetic energy of the studied molecules, respectively. Figures 4 and 5 are the binding energy and the adsorption energy of the molecules on the surface of the used metal, respectively.

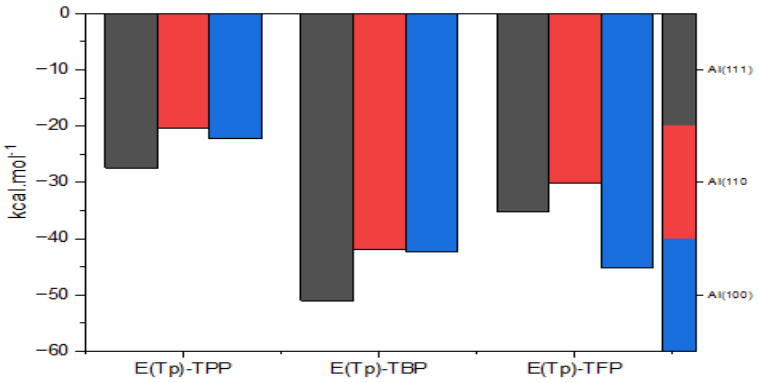

Figure 2: Total potential energy in kcal/mol on the surface of different Als.

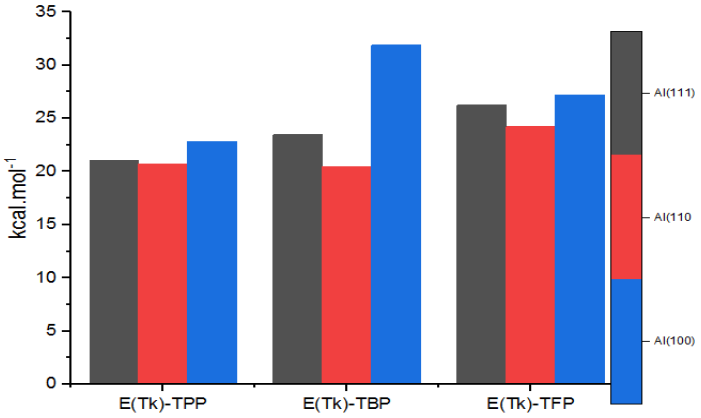

Figure 3: Total kinetic energy in kcal/mol on the surface of different Als.

The kinetic energy is relatively lower for Al(110) and Al(100) compared to Al(111), with values of 20.741 ± 0.02 and 22.836 ± 0.4, respectively, in comparison to 21.057 ± 0.01 for Al(111). This suggests that the motion (vibration, rotation, translation) of molecules is slightly more restrained on certain on the surfaces [55]. The kinetic energy is notably higher for Al(100) (31.879 ± 0.1) compared to Al(111) (23.472 ± 0.0) and Al(110) (20.503 ± 0.5). This indicate that the TBP molecule promotes greater atomic or molecular movement on Al(100), potentially due to different interactions with the surface [5,28,56-59]. The kinetic energy for Al(100) (27.232 ± 1.1) is comparable to that of Al(111) (26.233 ± 0.0), but lower for Al(110) (24.214 ± 0.5). This suggests that TFP have a more uniform impact on the kinetic energy across the aluminium surfaces but with less variability compared to TBP [50]. The potential energy values are negative across all surfaces, indicating an attractive interaction between the inhibitor and the aluminium surfaces. The most negative value is on Al (111) (-27.439 ± 0.01), followed by Al(100) (-22.261 ± 0.4) and Al(110) (-20.479 ± 0.02). This suggests that TPP interacts most favourably with the Al (111) surface, promoting stronger adhesion [37,47]. The potential energy is more negative for all surfaces compared to TPP, with values of -50.995 ± 0.0 (Al (111)), -41.843 ± 0.5 (Al (110)), and -42.330 ± 0.1 (Al(100)). This suggests that TBP creates stronger attractive interactions with the aluminium surfaces, potentially indicating better corrosion inhibition properties according to Nyijime *et al.* and Iorhuna *et al.* [37,60]. The potential energy values for TFP are also negative, but somewhat less negative than TBP, with values of -35.2225 ± 0.0 (Al (111)), -30.222 ± 0.5 (Al(110)), and -45.225 ± 1.1 (Al(100)). Interestingly, TFP shows the most negative potential energy for the Al(100) surface, indicating stronger interactions with this orientation compared to Al(110) and Al(111). From the result of the kinetic and potential energy of the molecules presented in Table 3, TPP causes relatively less movement, especially on Al(110) and Al(100) surfaces.

TBP induces the highest kinetic energy, particularly on the Al(100) surface, which indicate effective inhibition. TFP induces a moderate kinetic energy level across the surfaces, with the least variation compared to TBP. Meanwhile, the results show a clear trend in the strength of interactions between the inhibitors and the aluminum surfaces. TBP consistently has the most negative potential energy, suggesting it forms the strongest bonds with the aluminum surfaces and thus may be the most effective inhibitor. TFP's potential energy is lower on Al(100), suggesting stronger inhibition on this surface compared to the others, while TPP has the least negative potential energy, indicating weaker interactions with the aluminium surfaces [61].

Figure 4 and 5 present the graphical binding energies and adsorption energies of the molecules on the surfaces of the aluminum use in the study, respectively.

Table 3: Energies of the surface interactions between the molecules and aluminium surfaces

TPP	**Al(111)**	**Al(110**	**Al(100)**
Binding	59.2590±0.01	48.8887±0.02	54.6998±0.4
Adsorption	-59.2590±0.01	-48.8887±0.02	-54.6998±0.4
TBP			
Binding	83.681±0.0	65.664±0.5	75.521±0.1
Adsorption	-83.681±0.0	-65.664±0.5	-75.521±0.1
TFP			
Binding	72.280±0.0	46.061±0.5	60.238±1.1
Adsorption	-72.280±0.0	-46.061±0.5	-60.238±1.1

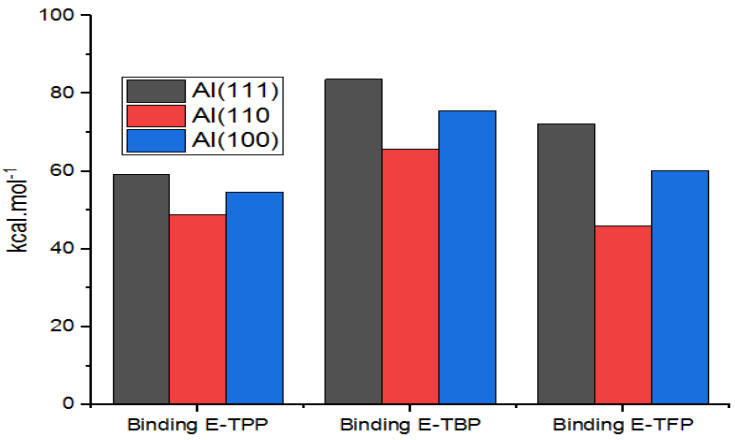

Figure 4: Binding energies of the molecules.

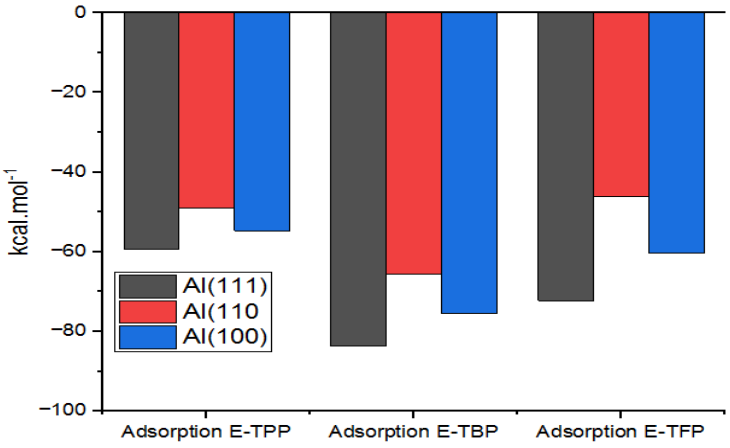

Figure 5: Adsorption energies of the molecules.

Based on the data presented in Table 2 for different surfaces of aluminium (Al(111), Al(110), Al(100)), the binding energies for the three molecules (TPP, TBP, and TFP) has a binding energy of 59.2590 (±0.01) kcal/(mol), which is stronger than 48.8887(±0.02) kcal/(mol) on Al(110). TBP on Al(111) has a binding energy of 83.681 (±0.0), the highest among all the molecules. While TFP on Al(111) has a binding energy of 2.280(±0.0) kcal/(mol). The trend in this result suggests that higher binding energy is generally associated with stronger attachment of the molecule to the surface, which can enhance the molecule's ability to resist corrosion by creating a more durable protective layer on the metal.: Adsorption energy represents the energy released when a molecule attaches to a surface [37]. Negative adsorption energy indicates a favourable interaction, where the molecule adheres strongly to the metal surface. For corrosion protection, molecules that exhibit high negative adsorption energy (more exothermic adsorption) tend to form a stable, protective layer that can reduce metal oxidation and corrosion. TPP has a -59.2590(±0.01) kcal/(mol) adsorption energy on Al(111), which is a strong adsorption compared to -48.8887 (±0.02) kcal/(mol) on Al(110). TBP shows a strong negative adsorption energy of -83.681(±0.0) kcal/(mol) on Al(111), which is more exothermic than TPP, suggesting a highly stable protective layer.

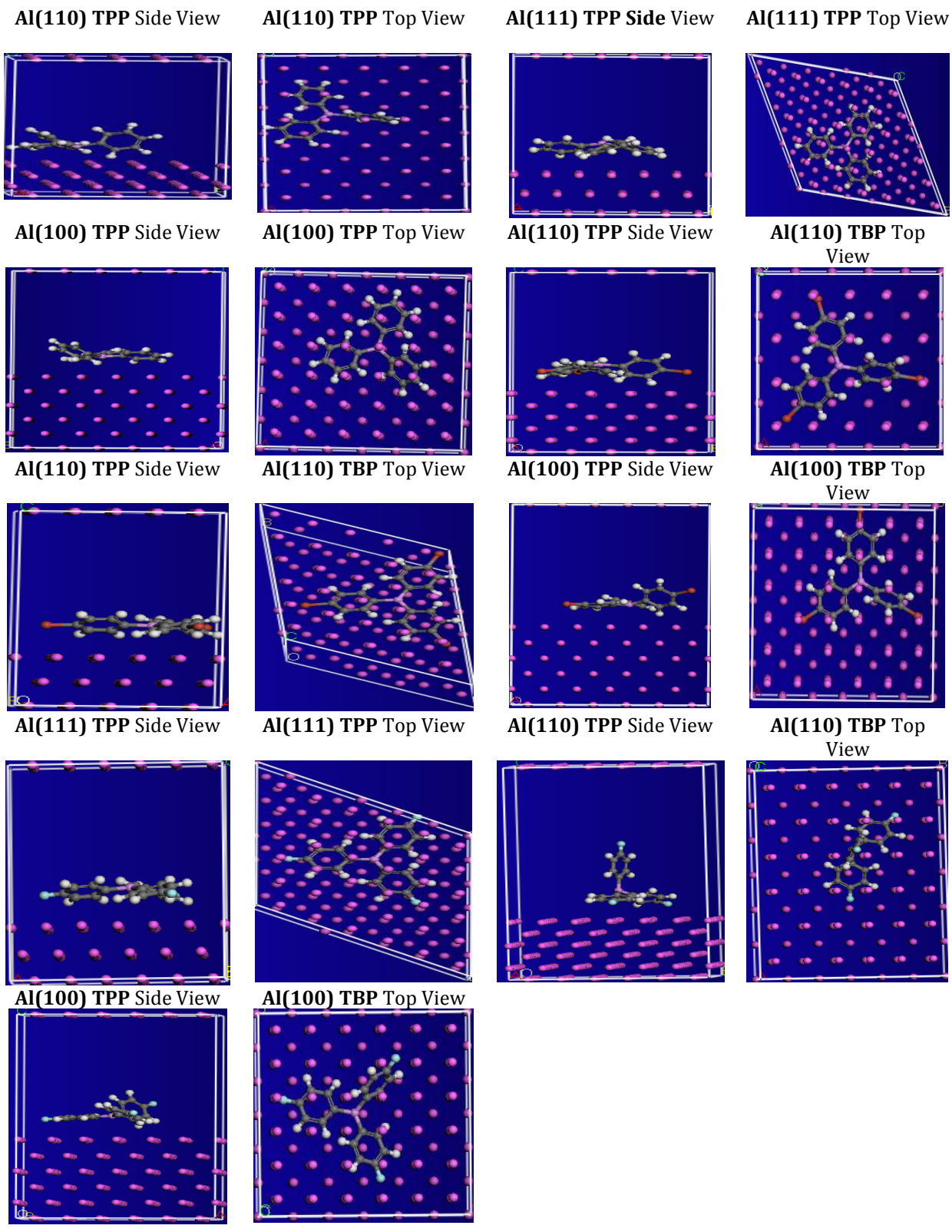

Figure 6: The pictorial representation of the simulation of triphenylphosphine (TPP).

TPP on Al(110)

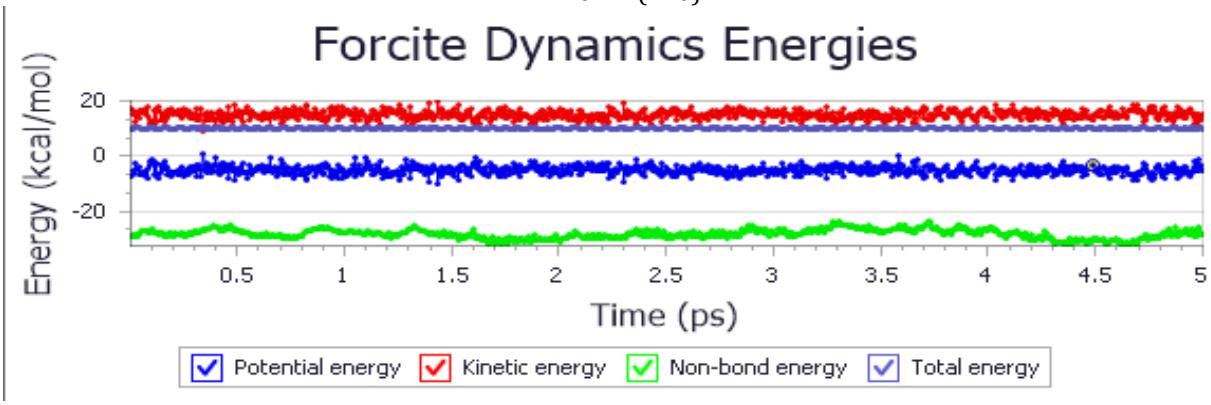

TPP on Al(111)

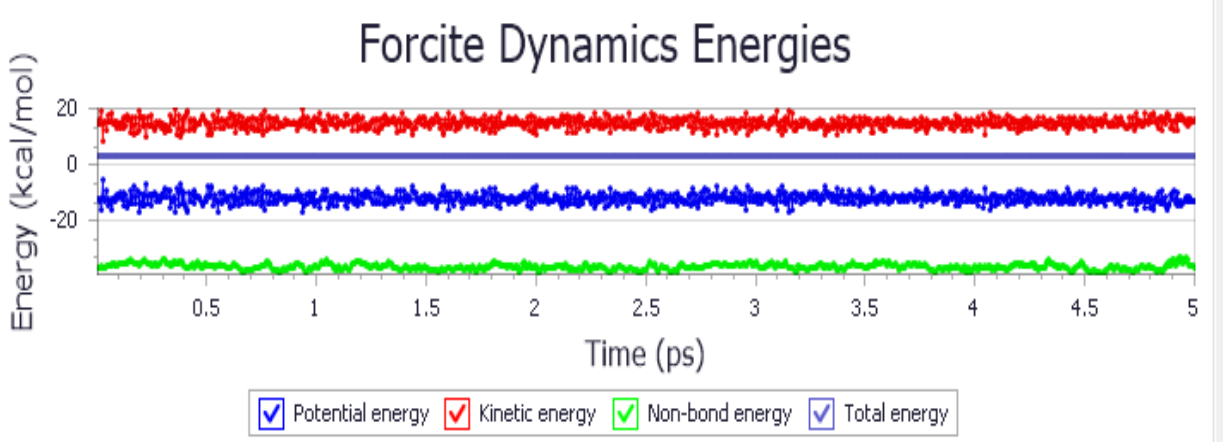

TPP on Al(100)

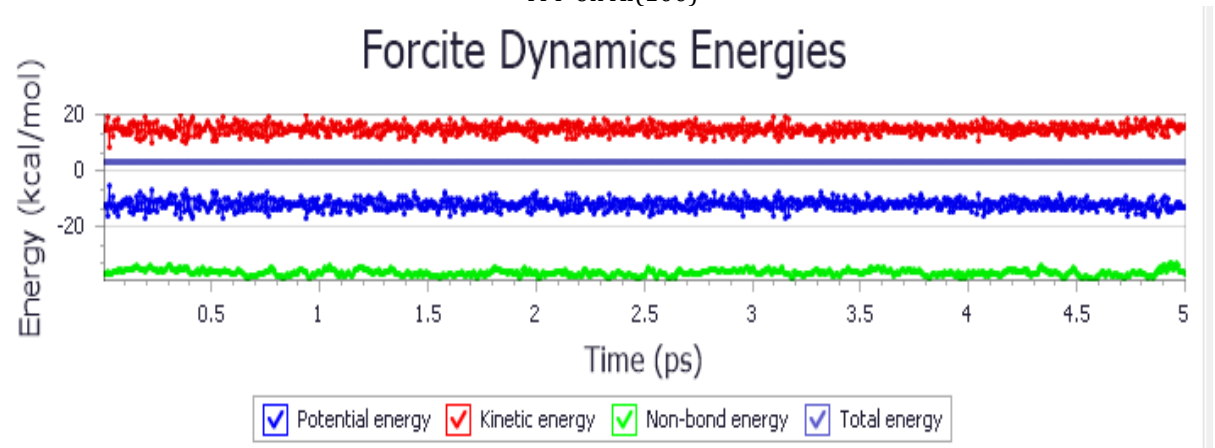

TBP on Al(110)

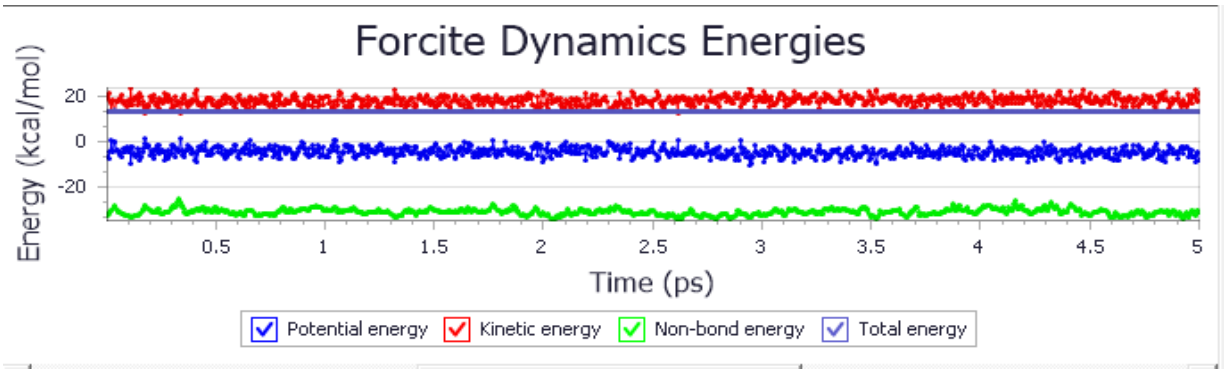

TBP on Al(111)

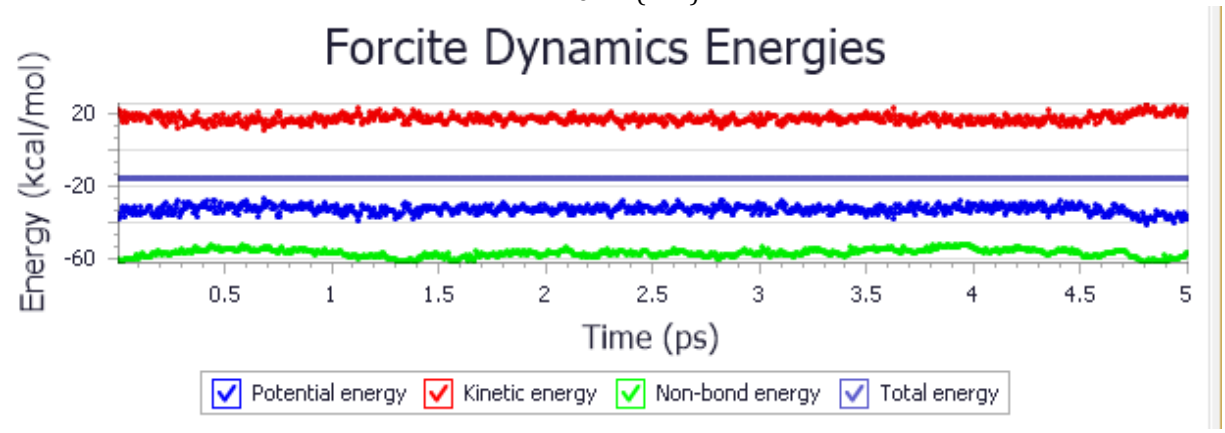

TBP on Al(100)

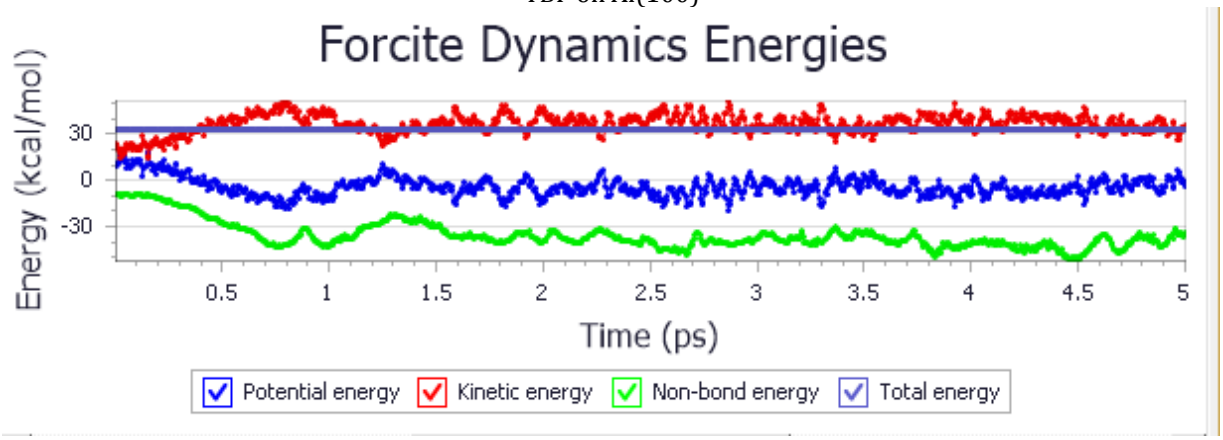

TFP on Al(111)

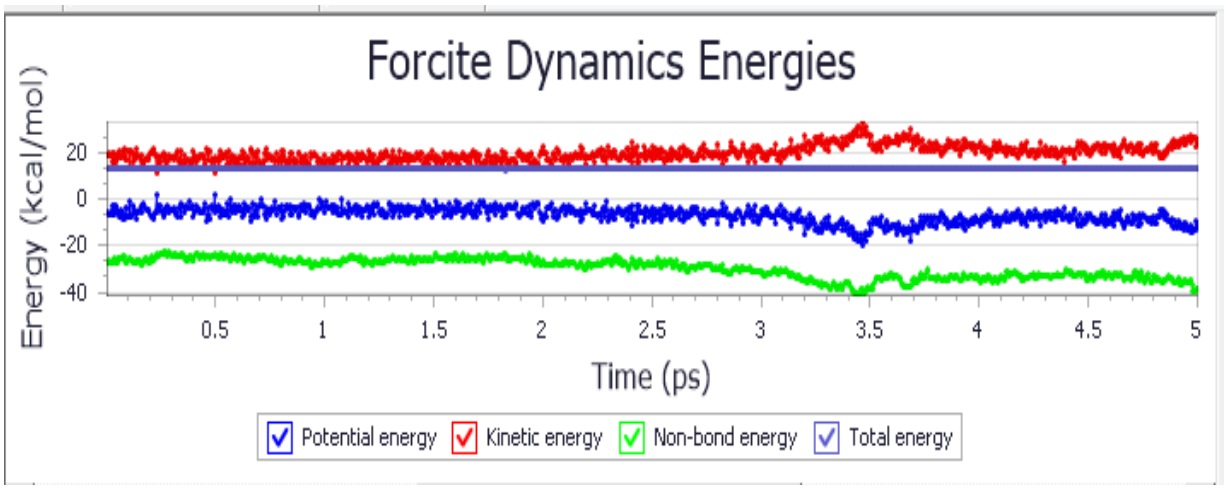

TFP on Al(110)

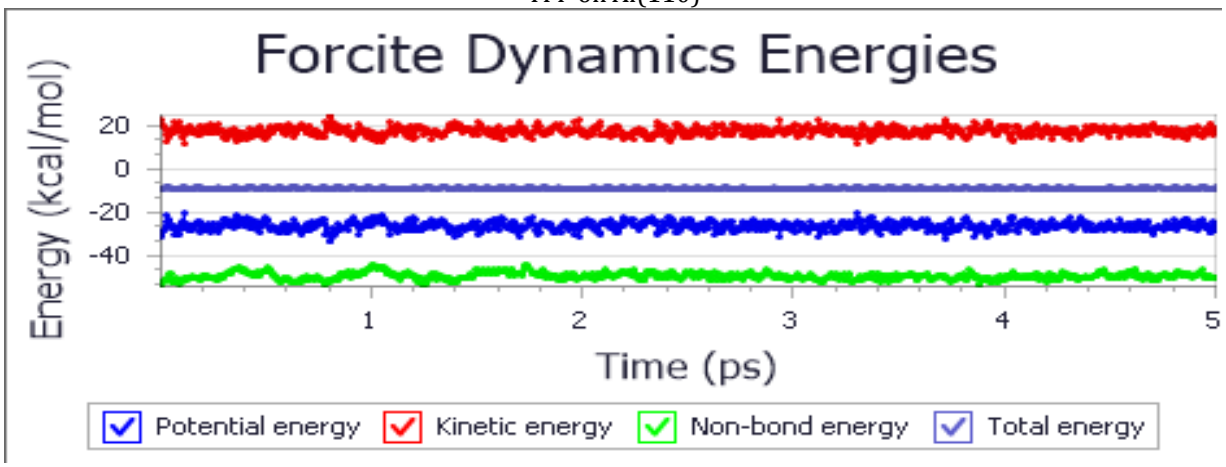

TFP on Al(100)

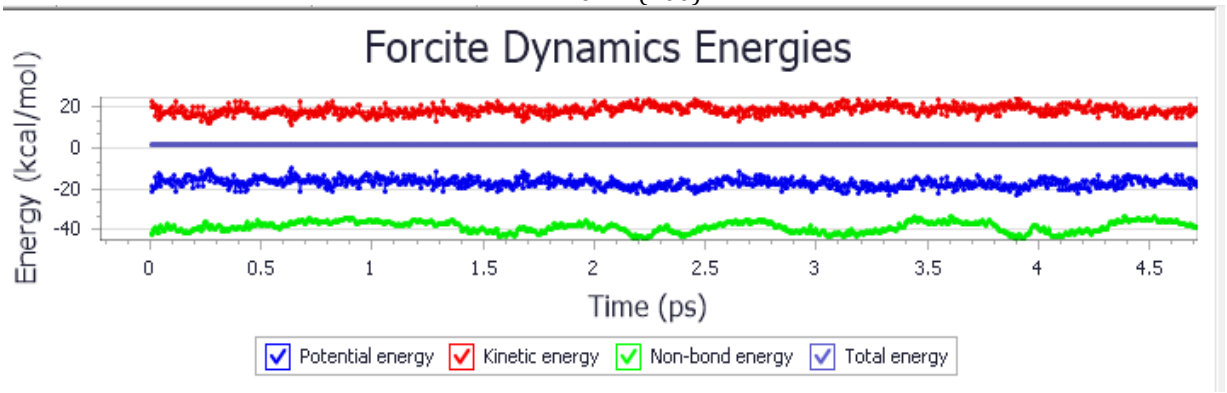

Figure 7: The graphical representation of the dynamic energies of the molecules ion the surfaces.

TFP shows a negative adsorption energy of -72.280 (±0.0) kcal/(mol) on Al(111), also suggesting a strong adsorption as the result of the simulation is presented in Figure 6.

The dynamic energies of the molecule is illustrated in Figure 7 which shows different energies of the molecule.

Conclusion

To sum up, this study highlights the corrosion inhibition potential of TPP, TBP, and TFP by evaluating their electronic properties and interaction energies with aluminum surfaces (Al(111), Al(110), and Al(100)). TPP exhibits the highest ability to donate electrons, with

favorable HOMO/LUMO energies, low ionization energy, and high nucleophilicity, making it the most effective electron donor and a promising corrosion inhibitor. TBP, while more electronegative and softer, shows stronger attractive interactions with the aluminum surfaces, particularly on Al(100), indicating its potential as a corrosion inhibitor, although it is less effective at donating electrons compared to TPP. TFP shows moderate corrosion inhibition ability, with its ability for back donation and moderate nucleophilicity, but its larger energy gap and lower electrophilicity reduce its overall reactivity. Kinetic energy after simulations reveal that TBP induces the highest kinetic energy, particularly on Al(100), suggesting strong molecular movement and effective inhibition. TPP causes less movement, especially on Al(110) and Al(100), while TFP has a more uniform impact across the surfaces. Overall, TBP exhibits the strongest interactions with the aluminum surfaces, as seconded by TFP and TPP. This suggests that TBP may offer the most robust corrosion protection. These findings underscore the importance of electron donation and molecular interaction strength in determining the effectiveness of corrosion inhibitors.

Orcid

Fater Iorhuna: 0000-0002-1018-198X
Abdullahi Muhammad Ayuba: 0000-0002-2295-8282
Thomas Aondofa Nyijime: 0000-0001-9537-1987

Reference

[1]. T. Nagalakshmi, A. Sivasakthi, Corrosion control, prevention and mitigation in oil & gas industry, *International Journal of Innovative Technology and Exploring Engineering (IJITEE)*, **2019**, *9*, 1568-1572. [Crossref], [Google Scholar], [Publisher]

[2]. B. Ran, Y. Qiang, X. Liu, L. Guo, A.G. Ritacca, I. Ritacco, X. Li, Excellent performance of amoxicillin and potassium iodide as hybrid corrosion inhibitor for mild steel in HCl environment: Adsorption characteristics and mechanism insight, *Journal of Materials Research and Technology*, **2024**, *29*, 5402-5411. [Crossref], [Google Scholar], [Publisher]

[3]. M. Palomar-Pardavé, M. Romero-Romo, H. Herrera-Hernández, M. Abreu-Quijano, N.V. Likhanova, J. Uruchurtu, J. Juárez-García, Influence of the alkyl chain length of 2 amino 5 alkyl 1, 3, 4 thiadiazole compounds on the corrosion inhibition of steel immersed in sulfuric acid solutions, *Corrosion Science*, **2012**, *54*, 231-243. [Crossref], [Google Scholar], [Publisher]

[4]. A. Zarrouk, B. Hammouti, T. Lakhlifi, M. Traisnel, H. Vezin, F. Bentiss, New 1H-pyrrole-2, 5-dione derivatives as efficient organic inhibitors of carbon steel corrosion in hydrochloric acid medium: electrochemical, XPS and DFT studies, *Corrosion Science*, **2015**, *90*, 572-584. [Crossref], [Google Scholar], [Publisher]

[5]. M. Boulhaoua, M. El Hafi, S. Zehra, L. Eddaif, A.A. Alrashdi, S. Lahmidi, L. Guo, J.T. Mague, H. Lgaz, Synthesis, structural analysis and corrosion inhibition application of a new indazole derivative on mild steel surface in acidic media complemented with DFT and MD studies, *Colloids and Surfaces A: Physicochemical and Engineering Aspects*, **2021**, *617*, 126373. [Crossref], [Google Scholar], [Publisher]

[6]. H. Lgaz, S. Masroor, M. Chafiq, M. Damej, A. Brahmia, R. Salghi, M. Benmessaoud, I.H. Ali, M.M. Alghamdi, A. Chaouiki, Evaluation of 2-mercaptobenzimidazole derivatives as corrosion inhibitors for mild steel in hydrochloric acid, *Metals*, **2020**, *10*, 357. [Crossref], [Google Scholar], [Publisher]

[7]. M. Rbaa, M. Galai, A.S. Abousalem, B. Lakhrissi, M.E. Touhami, I. Warad, A. Zarrouk, Synthetic, spectroscopic characterization, empirical and theoretical investigations on the corrosion inhibition characteristics of mild steel in molar hydrochloric acid by three novel 8-hydroxyquinoline derivatives, *Ionics*, **2020**, *26*, 503-522. [Crossref], [Google Scholar], [Publisher]

[8]. V. Barton, N. Fisher, G.A. Biagini, S.A. Ward, P.M. O'Neill, Inhibiting Plasmodium cytochrome bc1: a complex issue, *Current Opinion in Chemical Biology*, **2010**, *14*, 440-446. [Crossref], [Google Scholar], [Publisher]

[9]. C. Graebe, H. Caro, Ueber acridin, *Journal für Praktische Chemie*, **1870**, *158*, 183-185. [Crossref], [Google Scholar], [Publisher]
[10]. A.M. Ayuba, U. Umar, Modeling vitexin and isovitexin flavones as corrosion inhibitors for aluminium metal, *Karbala International Journal of Modern Science*, **2021**, *7*, 4. [Crossref], [Google Scholar], [Publisher]
[11]. U. Shehu, B. Usman, Corrosion inhibition of iron using silicate base molecules: A computational study, *Advanced Journal of Chemistry, Section A*, **2023**, *6*, 334. [Crossref], [Google Scholar], [Publisher]
[12]. H. Eagle, C. Washington, S.M. Friedman, The synthesis of homocystine, cystathionine, and cystine by cultured diploid and heteroploid human cells, *Proceedings of the National Academy of Sciences*, **1966**, *56*, 156-163. [Crossref], [Google Scholar], [Publisher]
[13]. N.A. Khudhair, I.M.H. Al-Mousawi, M.I. Ali, DFT-quantum chemical and experimental studies of eco-friendly approach to corrosion inhibition of stainless steel 316L in body fluid solution by dexamethasone drug, *Advanced Journal of Chemistry, Section A*, **2024**, 7, 868-882. [Crossref], [Publisher]
[14]. A.A. Siaka, N. Eddy, S. Idris, L. Magaji, Z. Garba, I. Shabanda, Quantum Chemical Studies of corrosion inhibition and adsorption potentials of Amoxicillin on mild steel in HCl solution, *International Journal of Modern Chemistry*, **2013**, *4*, 1-10. [Crossref], [Google Scholar], [Publisher]
[15]. C. Verma, M. Quraishi, E. Ebenso, I. Obot, A. El Assyry, 3-Amino alkylated indoles as corrosion inhibitors for mild steel in 1M HCl: Experimental and theoretical studies, *Journal of Molecular Liquids*, **2016**, *219*, 647-660. [Crossref], [Google Scholar], [Publisher]
[16]. D.K. Verma, Density functional theory (DFT) as a powerful tool for designing corrosion inhibitors in aqueous phase, *Advanced Engineering Testing*, **2018**, *87*. [Google Scholar], [Publisher]
[17]. A.A. Muhammad, N.A. Thomas, S. AbubakarMinjibir, N.U. Shehu, F. Iorhuna, Exploring the inhibition potential of carbamodithionic acid on Fe (111) surface: A theoretical study, *Journal of Engineering in Industerial Research*, **2024**, *4*, 201-210. [Crossref], [Google Scholar], [Publisher]
[18]. W.N. Al-Sieadi, O.H. Al-Jeilawi, N.A. Khudhair, A.N. Shamaya, N.A. Abdulrahman, Synthesis and characterization of heterocyclic derivatives to evaluate their efficiency as corrosion inhibitors for carbon steel in saline medium, *Advanced Journal of Chemistry, Section A*, **2025**, *8*, 209-219. [Crossref], [Google Scholar], [Publisher]
[19]. I. Lukovits, E. Kalman, F. Zucchi, Corrosion inhibitors—correlation between electronic structure and efficiency, *Corrosion*, **2001**, *57*, 3-8. [Crossref], [Google Scholar], [Publisher]
[20]. M. Belghiti, S. Echihi, A. Dafali, Y. Karzazi, M. Bakasse, H. Elalaoui-Elabdallaoui, L. Olasunkanmi, E. Ebenso, M. Tabyaoui, Computational simulation and statistical analysis on the relationship between corrosion inhibition efficiency and molecular structure of some hydrazine derivatives in phosphoric acid on mild steel surface, *Applied Surface Science*, **2019**, *491*, 707-722. [Crossref], [Google Scholar], [Publisher]
[21]. T.A. Nyijime, H.F. Chahul, A. Ayuba, F. Iorhuna, Theoretical investigations on thiadiazole derivatives as corrosion inhibitors on mild steel, *Advanced Journal of Chemistry-Section A*, **2023**, *6*, 141-154. [Crossref], [Google Scholar], [Publisher]
[22]. H. Kumar, V. Ramesh, J. Mohanbabu, A. Manogaran, A. Jayaraman, B. Siva Kumar, K. Ilango. Bio-orthogonal chemistry: Pioneering therapeutic precision in medicine, *Progress in Chemical and Biochemical Research*, **2024**, *7*, 430-452. [Crossref], [Publisher]
[23]. Thakur A. Kumar Computational insights into the corrosion inhibition potential of some pyridine derivatives: A DFT approach Eur. J. Chem. **2023**, 14(2), 246-25. [Google Scholar], [Publisher]
[24]. A.M. Ayuba, F. Iorhuna, T.A. Nyijim, H. Muhammadjamiu, S.M. Terna, T.O. Bello, Anticorrosion activities of cysteine on iron, aluminium and copper using density functional theory (DFT), *Jabirian Journal of Biointerface Research in Pharmaceutics and Applied Chemistry*, **2024**, *1*, 13-21. [Crossref], [Google Scholar], [Publisher]
[25]. L.T. Popoola, T.A. Aderibigbe, M.A. Lala, Mild steel corrosion inhibition in hydrochloric acid using cocoa pod husk-ficus exasperata: extract preparation optimization and

characterization, *Iranian Journal of Chemistry and Chemical Engineering*, **2022**, *41*, 482-492. [Crossref], [Google Scholar], [Publisher]
[26]. R.M. Kubba, N.M. Al-Joborry, Theoretical study of a new oxazolidine-5-one derivative as a corrosion inhibitor for carbon steel surface, *Iraqi Journal of Science*, **2021**, 1396-1403. [Crossref], [Google Scholar], [Publisher]
[27]. K.A.K. Al-Rudaini, K.A.S. Al-Saadie, Milk Thistle leaves aqueous extract as a new corrosion inhibitor for aluminum alloys in alkaline medium, *Iraqi Journal of Science*, **2021**, 363-372. [Crossref], [Google Scholar], [Publisher]
[28]. M.A. Mohammed, R.M. Kubba, Experimental Evaluation for the inhibition of carbon steel corrosion in salt and acid media by new derivative of quinolin-2-one, *Iraqi Journal of Science*, **2020**, 1861-1873. [Crossref], [Google Scholar], [Publisher]
[29]. S. Mammeri, N. Chafai, H. Harkat, R. Kerkour, S. Chafaa, Protection of steel against corrosion in acid medium using dihydropyrimidinone derivatives: experimental and DFT study, *Iranian Journal of Science and Technology, Transactions A: Science*, **2021**, *45*, 1607-1619. [Crossref], [Google Scholar], [Publisher]
[30]. F. Iorhuna, M.A. Ayuba, A.T. Nyijime, M. Sani, H. Abdulmumini, J.O. Oyeyode, A comparative computational stimulation studies on corrosion inhibition and adsorptive, *Eurasian Journal of Science and Technology*, **2024**, *4*. [Crossref], [Google Scholar], [Publisher]
[31]. T.V. Kumar, J. Makangara, C. Laxmikanth, N.S. Babu, Computational studies for inhibitory action of 2-mercapto-1-methylimidazole tautomers on steel using of density functional theory method (DFT), *International Journal of Computational and Theoretical Chemistry*, **2016**, *4*, 1-6. [Crossref], [Google Scholar], [Publisher]
[32]. T. Esan, O. Oyeneyin, A. Olanipekun, N. Ipinloju, Corrosion inhibitive potentials of some amino acid derivatives of 1, 4-naphthoquinone–DFT calculations, *Advanced Journal of Chemistry, Section A*, **2022**, *5*, 263. [Crossref], [Google Scholar], [Publisher]
[33]. R.M. Kubba, N.M. Al-Joborry, N.J. Al-lami, Theoretical and experimental studies for inhibition potentials of imidazolidine 4-one and oxazolidine 5-one derivatives for the corrosion of carbon steel in Sea Water, *Iraqi Journal of Science*, **2020**, 2776-2796. [Crossref], [Google Scholar], [Publisher]
[34]. Z. Yavari, M. Darijani, M. Dehdab, Comparative theoretical and experimental studies on corrosion inhibition of aluminum in acidic media by the antibiotics drugs, *Iranian Journal of Science and Technology, Transactions A: Science*, **2018**, *42*, 1957-1967. [Crossref], [Google Scholar], [Publisher]
[35]. N.M. Al-Joborry, R.M. Kubba, Theoretical and experimental study for corrosion inhibition of carbon steel in salty and acidic media by a new derivative of imidazolidine 4-one, *Iraqi Journal of Science*, **2020**, 1842-1860. [Crossref], [Google Scholar], [Publisher]
[36]. S. John, J. Joy, M. Prajila, A. Joseph, Electrochemical, quantum chemical, and molecular dynamics studies on the interaction of 4-amino-4H, 3, 5-di (methoxy)-1, 2, 4-triazole (ATD), BATD, and DBATD on copper metal in 1N H2SO4, *Materials and corrosion*, **2011**, *62*, 1031-1041. [Crossref], [Google Scholar], [Publisher]
[37]. M. Belghiti, S. Echihi, A. Dafali, Y. Karzazi, M. Bakasse, H. Elalaoui-Elabdallaoui, L. Olasunkanmi, E. Ebenso, M. Tabyaoui, Computational simulation and statistical analysis on the relationship between corrosion inhibition efficiency and molecular structure of some hydrazine derivatives in phosphoric acid on mild steel surface, *Applied Surface Science*, **2019**, *491*, 707-722. [Crossref], [Google Scholar], [Publisher]
[38]. M.M. Kadhim, L.A.A. Juber, A.S. Al-Janabi, Estimation of the efficiency of corrosion inhibition by Zn-dithiocarbamate complexes: A theoretical study, *Iraqi Journal of Science*, **2021**, 3323-3335. [Crossref], [Google Scholar], [Publisher]
[39]. D. Glossman-Mitnik, Computational study of the chemical reactivity properties of the Rhodamine B molecule, *Procedia Computer Science*, **2013**, *18*, 816-825. [Crossref], [Google Scholar], [Publisher]
[40]. L.H. Madkour, I. Elshamy, Experimental and computational studies on the inhibition performances of benzimidazole and its derivatives for the corrosion of copper in nitric acid, *International Journal of Industrial*

Chemistry, **2016**, *7*, 195-221. [Crossref], [Google Scholar], [Publisher]
[41]. A.M. Ayuba, T.A. Nyijime, S.A. Minjibir, F. Iorhuna, Adsorption monitoring of triflouroaceticacid, pentadecyl ester and pentadecanoic acid, 14-methyl-, methyl ester on Fe (110): using DFT and molecular simulation, *Eurasian Journal of Science and Technology*, **2024**, *4*, 105-116. [Crossref], [Google Scholar], [Publisher]
[42]. G. Kılınççeker, M. Baş, F. Zarifi, K. Sayın, Experimental and computational investigation for (E)-2-hydroxy-5-(2-benzylidene) aminobenzoic acid schiff base as a corrosion inhibitor for copper in acidic media, *Iranian Journal of Science and Technology, Transactions A: Science*, **2021**, *45*, 515-527. [Crossref], [Google Scholar], [Publisher]
[43]. J. Chen, X. Hu, J. Cui, Shikonin, vitamin K3 and vitamin K5 inhibit multiple glycolytic enzymes in MCF-7 cells, *Oncology Letters*, **2018**, *15*, 7423-7432. [Crossref], [Google Scholar], [Publisher]
[44]. H.A. AlMashhadani, K.A. Saleh, Electrochemical deposition of hydroxyapatite co-substituted by Sr/Mg coating on Ti-6Al-4V ELI dental alloy post-MAO as anti-corrosion, *Iraqi Journal of Science*, **2020**, 2751-2761. [Crossref], [Google Scholar], [Publisher]
[45]. L. Afandiyeva, V. Abbasov, L. Aliyeva, S. Ahmadbayova, E. Azizbeyli, H.M. El-Lateef Ahmed, Investigation of organic complexes of imidazolines based on synthetic oxy-and petroleum acids as corrosion inhibitors, *Iranian Journal of Chemistry and Chemical Engineering*, **2018**, *37*, 73-79. [Crossref], [Google Scholar], [Publisher]
[46]. T.A. Nyijime, H.F. Chahul, A. Ayuba, F. Iorhuna, Theoretical investigations on thiadiazole derivatives as corrosion inhibitors on mild steel, *Advanced Journal of Chemistry-Section A*, **2023**, *6*, 141-154. [Crossref], [Google Scholar], [Publisher]
[47]. H. Jafari, F. Mohsenifar, K. Sayin, Effect of alkyl chain length on adsorption behavior and corrosion inhibition of imidazoline inhibitors, *Iranian Journal of Chemistry and Chemical Engineering (IJCCE)*, **2018**, *37*, 85-103. [Crossref], [Google Scholar], [Publisher]
[48]. S. Elmi, M.M. Foroughi, M. Dehdab, M. Shahidi-Zandi, Computational evaluation of corrosion inhibition of four quinoline derivatives on carbon steel in aqueous phase, *Iranian Journal of Chemistry and Chemical Engineering (IJCCE)*, **2019**, *38*, 185-200. [Crossref], [Google Scholar], [Publisher]
[49]. L.T. Popoola, T.A. Aderibigbe, M.A. Lala, Mild steel corrosion inhibition in hydrochloric acid using cocoa pod husk-ficus exasperata: extract preparation optimization and characterization, *Iranian Journal of Chemistry and Chemical Engineering*, **2022**, *41*, 482-492. [Crossref], [Google Scholar], [Publisher]
[50]. R.M. Kubba, N.M. Al-Joborry, Theoretical study of a new oxazolidine-5-one derivative as a corrosion inhibitor for carbon steel surface, *Iraqi Journal of Science*, **2021**, 1396-1403. [Crossref], [Google Scholar], [Publisher]
[51]. A.B. Adegoke, R.A. Adepoju, A.T.A. Khan, Molecular dynamic (MD) simulation and modeling the bio-molecular structure of human UDP glucose-6-dehydrogenase isoform 1 (hUGDH) related to prostate cancer, *Basrah Journal of Science*, **2020**, *38*, 448-466. [Crossref], [Google Scholar], [Publisher]
[52]. T.A. Nyijime, P. Kutshak, H. Chahul, A.M. Ayuba, F. Iorhuna, V. Hudu, Theoretical investigation of aluminum corrosion inhibition using chalcone derivatives, *Mediterranean Journal of Chemistry*, **2024**, *14*, 58-68. [Crossref], [Google Scholar], [Publisher]
[53]. K. Chinthapally, B.S. Blagg, B.L. Ashfeld, Syntheses of symmetrical and unsymmetrical lysobisphosphatidic acid derivatives, *The Journal of organic chemistry*, **2022**, *87*, 10523-10530. [Crossref], [Google Scholar], [Publisher]
[54]. H. Takahashi, S. Nomura, Effects of hydrogen peroxide on chemical mechanical polishing of copper surface: Exploration of reaction pathways with molecular dynamics simulation and activation energies calculation, *Tribology Online*, **2024**, *19*, 194-208. [Crossref], [Google Scholar], [Publisher]
[55]. L. Guo, M. Zhu, J. Chang, R. Thomas, R. Zhang, P. Wang, X. Zheng, Y. Lin, R. Marzouki, Corrosion inhibition of N80 steel by newly synthesized imidazoline based ionic liquid in 15% HCl medium: experimental and theoretical investigations, *International Journal of Electrochemical Science*, **2021**, *16*, 211139. [Crossref], [Google Scholar], [Publisher]

[56]. H. Lgaz, S. Masroor, M. Chafiq, M. Damej, A. Brahmia, R. Salghi, M. Benmessaoud, I.H. Ali, M.M. Alghamdi, A. Chaouiki, Evaluation of 2-mercaptobenzimidazole derivatives as corrosion inhibitors for mild steel in hydrochloric acid, *Metals*, **2020**, *10*, 357. [Crossref], [Google Scholar], [Publisher]
[57]. D. Glossman-Mitnik, Computational study of the chemical reactivity properties of the Rhodamine B molecule, *Procedia Computer Science*, **2013**, *18*, 816-825. [Crossref], [Google Scholar], [Publisher]
[58]. A. Nahlé, R. Salim, F. El Hajjaji, M. Aouad, M. Messali, E. Ech-Chihbi, B. Hammouti, M. Taleb, Novel triazole derivatives as ecological corrosion inhibitors for mild steel in 1.0 M HCl: experimental & theoretical approach, *RSC advances*, **2021**, *11*, 4147-4162. [Crossref], [Google Scholar], [Publisher]
[59]. F. Iorhuna, S. Adulfatah, A.M. Ayuba, Quinazoline derivatives as corrosion inhibitors on aluminium metal surface: A theoretical study, *Advanced Journal of Chemistry-Section A*, **2023**, *6*, 71-84. [Crossref], [Google Scholar], [Publisher]
[60]. S. Junaedi, A.A. Al-Amiery, A. Kadihum, A.A.H. Kadhum, A.B. Mohamad, Inhibition effects of a synthesized novel 4-aminoantipyrine derivative on the corrosion of mild steel in hydrochloric acid solution together with quantum chemical studies, *International journal of molecular sciences*, **2013**, *14*, 11915-11928. [Crossref], [Google Scholar], [Publisher]
[61]. F. Iorhuna, A.S. Muhammad, M. Abdullahi Ayuba**,** Quinazoline derivatives as corrosion inhibitors on aluminium metal surface: A theoretical Study, *Advanced Journal of Chemistry-Section A*, **2023**, 6, 71-84 [Crossref], [Google Scholar], [Publisher]
[62]. F. Iorhuna, A.M. Ayuba, T. Nyijime, M. Shuaibu, A DFT and molecular dynamic (MD) simulation on the adsorption of vidarabine as a potential inhibitor on the al metal surface, *Advanced Journal of Chemistry-Section A*, **2023**, *6*, 380. [Crossref], [Google Scholar], [Publisher]